Journal of Materials Chemistry

Cite this: *J. Mater. Chem.*, 2011, **21**, 5629

www.rsc.org/materials

**PAPER**

# Chain scission resists for extreme ultraviolet lithography based on high performance polysulfone-containing polymers†

**Kirsten J. Lawrie,[a] Idriss Blakey,[a] James P. Blinco,‡[a] Han Hao Cheng,[a] Roel Gronheid,[b] Kevin S. Jack,[c] Ivan Pollentier,[b] Michael J. Leeson,[bd] Todd R. Younkin[d] and Andrew K. Whittaker*[a]**

***Received 30th September 2010, Accepted 7th February 2011***
**DOI: 10.1039/c0jm03288c**



A series of polymers with a comb architecture were prepared where the poly(olefin sulfone) backbone was designed to be highly sensitive to extreme ultraviolet (EUV) radiation, while the well-defined poly(methyl methacrylate) (PMMA) arms were incorporated with the aim of increasing structural stability. It is hypothesized that upon EUV radiation rapid degradation of the polysulfone backbone will occur leaving behind the well-defined PMMA arms. The synthesized polymers were characterised and have had their performance as chain-scission EUV photoresists evaluated. It was found that all materials possess high sensitivity towards degradation by EUV radiation ($E_0$ in the range 4–6 mJ cm$^{-2}$). Selective degradation of the poly(1-pentene sulfone) backbone relative to the PMMA arms was demonstrated by mass spectrometry headspace analysis during EUV irradiation and by grazing-angle ATR-FTIR. EUV interference patterning has shown that materials are capable of resolving 30 nm 1 : 1 line : space features. The incorporation of PMMA was found to increase the structural integrity of the patterned features. Thus, it has been shown that terpolymer materials possessing a highly sensitive poly(olefin sulfone) backbone and PMMA arms are able to provide a tuneable materials platform for chain scission EUV resists. These materials have the potential to benefit applications that require nanopattering, such as computer chip manufacture and nano-MEMS.

## Introduction

For more than 30 years the density of circuit elements on microchips has doubled roughly every 12 to 18 months. This has resulted in ever smaller, faster and cheaper computing and storage devices. Recent advances in lithographic processes have enabled the production of cutting edge microelectrical mechanical (MEMS)[1] and microfluidic devices.[2] Such continued advances in the production of nano-scale devices rely on improvements in the patterning capabilities of optical lithography. It is now recognised that the traditional technique for printing many circuit patterns, optical lithography, which is based on refractive optics (lenses), cannot continue to sustain such rapid growth. The current leading candidate for a successor, extreme ultraviolet (EUV) lithography, which uses a 13.5 nm wavelength light source, is theoretically capable of meeting the requirements of the 22 nm node and beyond. However, in order for this technology to fulfill the demands of high-volume production there are number of key challenges that remain to be resolved including the development of photoresists capable of simultaneously meeting industry requirements for sensitivity, resolution and line edge roughness (LER).[3]

Currently, photoresist technology relies heavily on the use of photoacid generators (PAGs) to chemically amplify the response of the resist formulation to the incident radiation, thus allowing cost-effective device manufacture. However, it has recently been shown that the diffusive path-length of the protons (and counter-ions) generated by the PAG in chemically amplified resist (CAR) systems is in the range of 11–25 nm,[4] which is a significant distance when compared with the target dimensions of EUV lithography (<22 nm). This results in blurring of the printed image[5] and is thought to be a major cause of the LER observed in chemically amplified systems.[6,7] Hence, acid diffusion will eventually limit the resolution of the process. Therefore, it is generally accepted that current chemically amplified resist systems lack the ability to simultaneously meet the resolution, LER and

[a]*The University of Queensland, Australian Institute for Bioengineering and Nanotechnology and Centre for Advanced Imaging, St Lucia, 4072, Queensland, Australia. E-mail: a.whittaker@uq.edu.au*
[b]*Imec, Kapeldreef 75, B-3001, Leuven, Belgium*
[c]*The University of Queensland, Centre for Microscopy and Microanalysis, St Lucia, 4072, Queensland, Australia*
[d]*Intel Corporation, Hilsboro, Oregon, 97124, USA*

† Electronic supplementary information (ESI) available: Contrast curves with a variety of developers for materials **2** and **3a**, SEM images of electron beam damage under high magnification. See DOI: 10.1039/c0jm03288c

‡ Current address: Preparative Macromolecular Chemistry, Institut für Technische Chemie und Polymerchemie, Universität Karlsruhe (TH)/Karlsruhe Institute of Technology (KIT), Engesserstr. 18, 76128 Karlsruhe, Germany.

sensitivity requirements for EUV lithography.[6,8] For this reason, there is a need to develop resist materials that do not rely on the generation of acids to meet sensitivity requirements. It has been shown that chain-scission materials show improved LER and resolution over CAR materials. This comes at the cost of sensitivity, however, with these systems requiring higher exposure doses.[9]

It was shown by Jack *et al.*[10] using a qualitative structure–property relationship (QSPR) model that certain functional groups such as sulfones and carbonates[11] are highly sensitive to degradation by 70 eV electrons. This is comparable to the energy of secondary electrons that will be formed during irradiation with 13.5 nm photons.[12] Moreover, it has long been established that sulfone-containing polymers, such as poly(olefin sulfone)s, are susceptible to degradation by ionising radiation such as electron beams and γ-rays.[13] The high sensitivity of these materials is a result of the scission of the relatively weak carbon–sulfur bonds in the polymer backbone. The rate of degradation is dependent on a number of factors, one of which is the ceiling temperature ($T_c$) of the material. This is the temperature at which the rates of propagation and depropagation reactions are equal. Above this temperature, the polymerisation reaction is no longer favourable and the depolymerisation reaction takes place more rapidly. Thus the polymers have a propensity to 'unzip' to the parent monomers, *i.e.* $SO_2$ and the olefin.[14] Generally, the ceiling temperatures for poly(olefin sulfone)s are at or below room temperature.[15] When considered in terms of a photoresist material, the 'unzipping' process will occur at temperatures above $T_c$ once radicals are generated from chain scission processes during irradiation. This ability to easily degrade to parent monomers following irradiation could be considered 'self-development' removing the need for solvents and extra production steps. Due to this high sensitivity, a number of polysulfones have been investigated for use as electron beam lithographic resists.[16] However, no studies to date have been conducted on the sensitivity of these materials to EUV radiation.

A potential drawback of the sulfone-based materials is that their thermal stability and etch resistance during later processing steps have been reported to be below acceptable levels.[17] Thus, investigations towards improving these properties have involved the incorporation of etch-resistant[18] or thermally stable[17] moieties into various poly(olefin sulfone) backbones. More recently, studies have been conducted on comb-shaped terpolymers possessing a radiation sensitive poly(olefin sulfone) backbone and radiation resistant side arms.[19,20] Incorporation of these radiation-resistant moieties led to sensitive materials[20] with improved etch resistance and thermal properties which were able to be used as multilayer systems for direct-write electron beam applications.

In this work a series of novel polymers with a comb-shaped architecture have been prepared. The synthetic methodologies employed in this study show a new approach to the design and synthesis of poly(olefin sulfone) terpolymer materials. In this investigation, olefin-terminated side arms of well defined molecular weights were synthesised by atom transfer radical polymerisation (ATRP) and then subsequently incorporated into a poly(olefin sulfone) backbone. Such an approach allows ease in tailoring both the molecular weight and the chemical nature of the side arms, because ATRP is compatible with a wide range of monomers. This translates to the ability to tune the properties of the final material. The polymer backbone has been designed to undergo rapid photodegradation upon exposure to EUV light, similar to sulfone resists previously synthesised and reported by our group.[21] The arms of the comb polymer have been selected to impart structural stability in the bulk of the resist, but will still be readily removed from irradiated areas by development. Due to the reported high sensitivity of poly(olefin sulfones) to EUV photons, poly(pentene sulfone) was selected as the backbone polymer, while the more robust poly(methyl methacrylate) (PMMA) has been selected for the arms. PMMA was chosen as an initial model due to its ease of characterisation, however, efforts are currently underway in our laboratories to synthesise the next generation of structures incorporating high $T_g$ and etch resistant moieties. In this study, the preferential degradation of the poly(olefin sulfone) backbone compared with the PMMA arms has been assessed, as has the lithographic performance of the polymers.

## Experimental

### Materials

Allyl bromoisobutyrate (Sigma-Aldrich, 98%), copper(I) bromide (Sigma-Aldrich, 99.999%), aluminium oxide (Sigma-Aldrich, activated basic, Brockmann I), sulfur dioxide (BOC Australia) and *tert*-butylhydroperoxide (Sigma-Aldrich, 5.0–6.0 M in decane), toluene (Ajax Finechem), dichloromethane (Merck), *n*-hexane (Merck), acetone (Merck) and methanol (Merck) were used as received. Methyl methacrylate (Sigma-Aldrich, 99% contains ≤30 ppm monomethyl ether hydroquinone as inhibitor) was filtered through a plug of basic alumina prior to reaction to remove inhibitor and 1-pentene (Sigma-Aldrich, 98%) was distilled under vacuum to remove any peroxides that may be present.

### Polymer synthesis

**General procedure for synthesis of allyl-terminated poly(methyl methacrylate) macromonomers *via* ATRP (1a–c).** MMA monomer (2.5 mL), allyl 2-bromoisobutyrate (ABIB), *N*-(*n*-hexyl)-2-pyridylmethaneimine ligand (prepared by a reported procedure[22]) and toluene (2.5 mL) were placed in a Schlenk flask and degassed by purging argon through the solution for 10 min. Cu(I)Br was added under positive pressure and the solution degassed by purging with argon for a further 5 min at room temperature, before being placed in an oil bath at 90 °C. After the required time, the reaction was removed from the heat and diluted with DCM. Catalyst residues were removed by filtering the solution through a column of basic alumina and the polymers were isolated by precipitation into cold hexane. The ratio of monomer : initiator : ligand : Cu(I)Br was $x$ : 1 : 2 : 1, where '$x$' is (desired $M_w$ of the polymer)/($M_w$ MMA): (**1a**)—(1.6 g, 67%), SEC analysis: $M_w$ = 3500 Da, $M_n$ = 2700 Da, $Đ_M$ 1.27; $M_n$ found from $^1$H NMR end group analysis = 3200 Da; $\delta_H$ (400 MHz, $CDCl_3$) 5.9 (1H, m, ABIB allyl CH), 5.23 (2H, q, ABIB allyl=$CH_2$), 4.5 (2H, d, ABIB allyl $CH_2O$), 3.55 (s, PMMA $OCH_3$), 1.7–3.0 (br m, PMMA backbone $CH_2$), 0.8–1.4 (br m, PMMA backbone $CH_3$). Thermal analysis: $T_g$ = 88 °C. (**1b**)—(1.1 g, 47%), SEC analysis: $M_w$ = 5600 Da, $M_n$ = 4700 Da, $Đ_M$ 1.19; $M_n$ found from $^1$H NMR end group analysis = 5200 Da; $\delta_H$

 

(400 MHz, $CDCl_3$) as for (**1a**); thermal analysis: $T_g$ = 95 °C. (**1c**)—(1.3 g, 55%), SEC analysis: $M_w$ = 12 650 Da, $M_n$ = 10 000 Da, $Đ_M$ 1.25; $M_n$ found from $^1$H NMR end group analysis = 11 200 Da; $\delta_H$ (400 MHz, $CDCl_3$) as for (**1a**); thermal analysis: $T_g$ = 113 °C.

**Synthesis of poly(1-pentene sulfone) (2)[21].** 1-Pentene (1 mL, 9.15 × $10^{-3}$ mol) was distilled under vacuum into a sealable Schlenk flask. To this flask $SO_2$ (2 mL, 3.16 × $10^{-2}$ mol) was condensed and the solution was degassed *via* three freeze–pump–thaw cycles to remove residual oxygen. The solution was cooled to −78 °C in a dry ice/acetone bath and *tert*-butylhydroperoxide (*t*-BuOOH) (1 mol% based on 1-pentene, 5.5 M solution in decane) was introduced *via* gas tight syringe. The reaction was stirred at −78 °C for 2 h, before being warmed to room temperature to allow unreacted $SO_2$ to boil off. The residue was dissolved in acetone and precipitated into methanol. Yield (1.87 g, 80%). SEC analysis: $M_w$ = 1 019 000, $M_n$ = 431 400, $Đ_M$ = 2.36; $\delta_H$ (400 MHz, $CDCl_3$) 3.8–4 (br d, backbone $CH_2$), 3.3–3.4 (br s, backbone CH), 1.9, 2.0 (br d, α-$CH_2$), 1.6 (β-$CH_2$), 0.97 (br t, $CH_3$). Thermal analysis: $T_g$ = 85 °C.

**Synthesis of poly(1-pentene-*co*-PMMA sulfone) terpolymers (3a–d).** 1-Pentene (1 mL, 9.15 × $10^{-3}$ mol) was distilled under vacuum into a sealable flask containing allyl-terminated PMMA (**1**). To this flask, $SO_2$ (4 mL, 6.32 × $10^{-2}$ mol) was condensed and the solution was degassed by three freeze–pump–thaw cycles to remove residual oxygen. The solution was cooled to −78 °C in a dry ice/acetone bath and *tert*-butylhydroperoxide (*t*-BuOOH) (1 mol% based on total moles of olefin, 5.5 M solution in decane) was introduced *via* a gas-tight syringe. The reaction was stirred at −78 °C for 4 h before being warmed to room temperature to allow excess $SO_2$ to evaporate. The residue was dissolved in acetone and precipitated into methanol. A ratio of 5 mol% PMMA macromonomer (based on 1-pentene) was used for synthesis of material (**3a**) while a ratio of 10 mol% (based on 1-pentene) was used for materials **3b–d**. (**3a**)—SEC analysis: $M_w$ = 185 600 Da, $M_n$ = 90 000 Da, $Đ_M$ 2.06; $\delta_H$ (400 MHz, $CDCl_3$) 3.8–4 (br d, backbone $CH_2$), 3.58 (s, PMMA $OCH_3$), 3.3–3.4 (br s, backbone CH), 1.9, 2.0 (br d, α-$CH_2$), 1.7 (s, PMMA backbone $CH_2$), 1.6 (β-$CH_2$), 0.97 (br t, $CH_3$), 0.82 (br s, PMMA backbone $CH_3$). Thermal analysis: $T_g$ = 83.9 °C. (**3b**)—SEC analysis: $M_w$ = 231 400 Da, $M_n$ = 137 000 Da, $Đ_M$ 1.69; $\delta_H$ (400 MHz, $CDCl_3$) as for (**3a**). Thermal analysis: $T_g$ = 84.2 °C. (**3c**)—SEC analysis: $M_w$ = 158 800 Da, $M_n$ = 46 800 Da, $Đ_M$ 3.39; $^1$H NMR ($CDCl_3$): as for (**3a**). Thermal analysis: $T_g$ = 84.6 °C. (**3d**)—SEC analysis: $M_w$ = 100 300 Da, $M_n$ = 38 900 Da, $Đ_M$ 2.58; $\delta_H$ (400 MHz, $CDCl_3$) as for (**3a**). Thermal analysis: $T_g$ = 84.4 °C.

## Instrumentation

Thermal analysis was conducted on a Mettler Toledo DSC1 STAR$^e$ System from 25 °C to 150 °C at a heating rate of 10 °C $min^{-1}$ for PMMA samples and 25 °C to 300 °C at a heating rate of 20 °C $min^{-1}$ for polysulfone samples.

Nuclear magnetic resonance (NMR) spectra were acquired on a Bruker Avance 400 MHz spectrometer using $CDCl_3$ as the solvent and referenced to the residual $CHCl_3$ solvent peak at 7.25 ppm relative to TMS.

Gel permeation chromatography of allyl-terminated PMMA samples was carried out by dissolving the polymer in tetrahydrofuran (THF) to a concentration of 1 mg $mL^{-1}$ and filtering through a 0.45 μm PTFE syringe filter. Analysis of the molecular weight distributions of the polymers was accomplished using a Waters 2695 separations module, fitted with a Waters 410 refractive index detector maintained at 36 °C, a Waters 996 photodiode array detector, and two Ultrastyragel linear columns (7.8 × 300 mm) arranged in series. These columns were maintained at 40 °C for all analyses and are capable of separating polymers in a molecular weight range of 500 to 4 × $10^6$ Da with high resolution. All samples were eluted at a flow rate of 1.0 mL $min^{-1}$. Calibration was performed using narrow molecular weight polystyrene standards ($Đ_M$ typically 1.03–1.06) ranging from 500 to 2 × $10^6$. Data acquisition was performed using Empower software, and molecular weights were calculated relative to polystyrene standards.

Absolute molecular weights of poly(olefin sulfone) materials were determined using a Polymer Labs GPC50 Plus equipped with a dual-angle laserlight-scattering detector, a viscometer and a differential-refractive-index detector. HPLC grade dimethylacetamide (DMAc) containing 0.03 wt% LiCl was used as eluent at a flow rate of 1 mL $min^{-1}$. Separations were achieved using two PLGel Mixed B (7.8 × 300 mm) SEC columns connected in series held at a constant temperature of 50 °C. The triple detection system was calibrated using a 2 mg $mL^{-1}$ polystyrene standard molecular weight 110k in DMAc containing 0.03 wt% LiCl ($dn/dc$ = 0.160 and IV = 0.5809 mL $g^{-1}$).

## Analysis of photodegradation and lithographic evaluation

**Spin coating.** Thin films of the materials were coated onto HMDS primed 200 mm silicon wafers from propylene glycol methyl ether acetate (PGMEA) solutions (2 w/v% solutions). Wafers were spun at 1500 rpm and underwent a post-apply bake (PAB) of 120 °C for 60 s. Films of *ca.* 60 nm were obtained for all materials.

**Open frame 92 eV synchrotron exposures and GATR analysis.** Thin films of **3b** were irradiated at the Australian Synchrotron using the soft X-ray beamline tuned to a photon energy of 92 eV. Grazing angle attenuated total reflectance FTIR (GATR-FTIR) was conducted on a Thermo Nicolet FTIR spectrometer using a Harrick grazing angle attenuated total reflectance accessory fitted with a germanium internal reflective element and MIR polarizers. To maximise the signal the polarisation of the incident beam was set to parallel to the silicon wafer surface.

**EUV contrast curve and headspace analysis.** Open-frame exposures by an EUV source were conducted at the Interuniversity Microelectronics Center (imec) using an experimental set-up supplied by EUV Technology (Martinez, US). The tool specifications and layout have been described elsewhere.[23] The term 'open frame' refers to irradiations conducted in the direct path of the photon beam with no mask present. For the contrast curve experiments post-exposure development was conducted by applying the desired developer on the wafer for 45 s before spinning dry.

Film-thickness measurements were carried out on a KLA-Tencor ASET-F5 ellipsometer using a wavelength range of 400–750 nm. The fitting model consisted of a single layer three parameter Cauchy model on silicon.

*In situ* headspace analysis of the gas evolved during irradiation of the polymers was conducted by moving the coated wafers through the path of the EUV beam to ensure a statistically relevant sample was obtained. The delivered dose was determined by the speed of wafer movement. Mass spectra of the evolved gases were measured using a mass spectrometer (Pfeiffer QMG422 RGA) using methods described previously.[23]

**EUV interference exposures and analysis.** EUV interference exposures were performed at the Paul Scherrer Institute (PSI) in Villigen, Switzerland by Dr Andreas Langer. The working principle of this setup has been described previously.[24] SEM images were taken on a Raith-150 (with Zeiss SEM column from Raith GmbH). The images were captured at 1 to 2 kV acceleration voltage and 30 μm aperture with working distance of 3 mm using in-lens detector mode. A MFP-3D (Asylum Research, USA) AFM with Etalon HA_NC (NT-MDT) cantilevers with a resonant frequency of 180 kHz and a spring constant of 5.6 N $m^{-1}$ was used for AFM measurements. AFM images were processed in image processing software, SPIP v.5 (Image Metrology A/S). Fast Fourier Transform (FFT) analysis was carried out on a 1.5 μm × 1.5 μm window. The peak positions that represent the pitches of resist patterns were determined from the line profiles of the peaks of the FFT maps. LER analysis was conducted using Summit (EUV Technology) software. The images were subjected to contrast enhancement (2–5% pixel saturation) and sharpening for the improvement of the edge contrast. Gaussian prefiltering was carried out prior to edge detection. The LER was carried out using polynomial edge detection with a threshold value of 0.3 and analysis length of 4 times the CD.

## Results and discussion

### Synthesis and characterisation

Macromonomers containing a polymerisable end group were synthesised using atom transfer radical polymerisation (ATRP) and were subsequently incorporated into a poly(1-pentene sulfone) backbone by copolymerisation with sulfur dioxide and pentene. The overall synthetic scheme for the study is shown in Scheme 1. In order to investigate the effect of varying the length of the arms of the final terpolymer product, a range of allyl-terminated PMMA macromonomers with well defined molecular weights was synthesised (materials: **1a** 2700 Da, **1b** 4800 Da, and **1c** 7600 Da) using an adapted literature procedure.[22]

Fig. 1(a) shows the $^1$H NMR spectrum of (**1a**), the 2.7k allyl-terminated PMMA macromonomer. From this spectrum it can be seen that there are broad peaks that can be assigned to PMMA in the 1–2 ppm region and peaks that can be assigned to the allyl end between 4.5 and 5.5 ppm, which indicates that the allyl end group moiety remains intact during the ATRP polymerisation process. In addition, good agreement was obtained between the $M_n$ determined using SEC and molecular weight calculated from the ratio of peak areas for end group allyl protons to methoxy protons in the $^1$H NMR spectrum (see the Experimental section for the integral values).

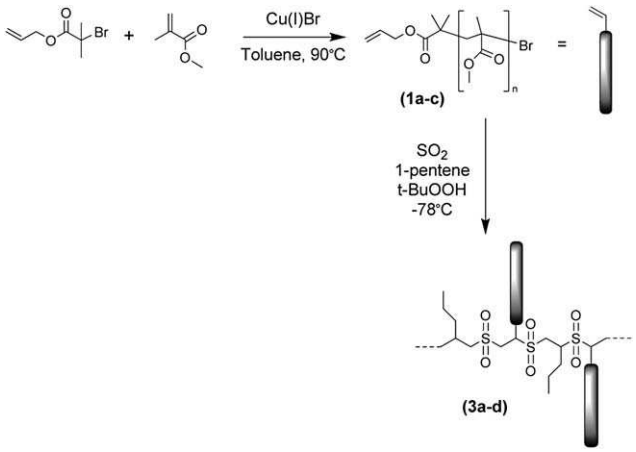


**Scheme 1** Synthesis of allyl-terminated PMMA macromers (**1a–c**) and poly(1-pentene-*co*-PMMA sulfone)s (**3a–d**) with a comb architecture.

Terpolymerisations were conducted using 5 and 10 mol% feed ratios (based on 1-pentene) of the desired allyl-terminated PMMA (materials **1a–c**). The crude products were purified by repeated precipitation into warm methanol, in order to solubilise any un-reacted macromonomer. The $^1$H NMR spectra of the terpolymer (**3b**) are shown in Fig. 1(c). Peaks assigned to PMMA and poly(1-pentene sulfone) repeat units in the terpolymer product can be clearly observed (see Experimental section for full peak assignments). Incorporation of the macromonomer into the terpolymer can be determined from the disappearance of the allyl peaks in the $^1$H NMR spectrum of (**3b**). The $^1$H NMR spectrum also exhibits no evidence of olefin–olefin linkages in the polymer backbone suggesting that an alternating sulfone olefin structure has been obtained.[25]

The amount of PMMA incorporated into the isolated product was determined using $^1$H NMR, whereby the area under the PMMA methoxy peak, at 3.6 ppm, was compared to that of the backbone polysulfone peaks at 3.9 ppm (Table 1). It was found

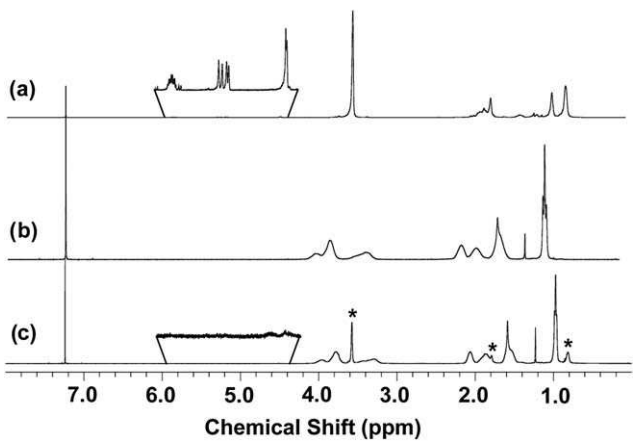


**Fig. 1** $^1$H NMR spectra of (a) allyl-terminated PMMA (**1a**), expansion shows allyl peaks, (b) poly(1-pentene sulfone) (**2**) and (C) poly(1-pentene-*co*-PMMA sulfone) 30 wt% 2k PMMA (**3b**), expansion shows allyl peaks are absent, indicating that no free macromonomer is present. Asterisks indicate most prominent peaks due to PMMA.

**Table 1** Molecular weight and thermal properties of materials prepared in this study

| Material code | PMMA $M_n$[a] | PMMA feed ratio (mol%) | No. % PMMA in product[b] | Wt% PMMA in product | Number of PMMA units per chain | $M_n$[c]/Da | $Đ_M$[d] | $T_g$/°C |
|---|---|---|---|---|---|---|---|---|
| **2** | — | — | — | — | 0 | 46 500 | 2.42 | 85 |
| **3a** | 2700 (**1a**) | 5 | 0.4 | 7 | 2 | 90 000 | 2.06 | 84 |
| **3b** | 2700 (**1a**) | 10 | 0.9 | 23 | 12 | 137 000 | 1.69 | 84 |
| **3c** | 4800 (**1b**) | 10 | 1.0 | 42 | 4 | 46 900 | 3.39 | 85 |
| **3d** | 7600 (**1c**) | 10 | 0.6 | 29 | 2 | 38 900 | 2.58 | 84 |

[a] Obtained using a THF SEC system calibrated using narrow molecular weight polystyrene standards. [b] Calculated from $^1$H NMR. [c] Obtained using triple detection on a DMAc SEC system. [d] $Đ_M = M_w/M_n$ obtained using triple detection on a DMAc SEC system.



that approximately 10% of the PMMA in the feed was incorporated into the isolated products (**3a–d**) (Table 1). Incomplete incorporation of the allyl-terminated PMMA in the feed was probably due to differences in the reactivity of 1-pentene and allyl-terminated PMMA towards copolymerisation with $SO_2$. It has previously been shown that the yield of poly(olefin sulfone)s from the reactions of allyl cinnamate[26] and allyl alcohol[27] with sulfur dioxide is lower than that observed for 1-hexene.[27] This suggests that allyl monomers that possess an adjacent oxygen atom may be less reactive towards copolymerisation with $SO_2$. It is also possible that the steric factors associated with the PMMA macromer hinder the participation of the terminal allyl group in propagation reactions. Further evidence for this hypothesis is that product (**3d**), which contains the largest PMMA chain investigated (7.6k), only exhibited 6% incorporation rather than the 10% observed for smaller chains.

Table 1 also shows the $T_g$ values determined for the terpolymer products. The observed $T_g$ values were not found to deviate significantly from that of the polysulfone homopolymer (Table 1). This is most likely due to the $T_g$ of the PMMA macromonomers (**1a–c**, Table 1) being similar to that of the polysulfone homopolymer (Table 1).

## Lithographic evaluation

**Sensitivity studies.** The sensitivity of the terpolymer materials (**3a–d**) towards EUV radiation was evaluated by conducting open-frame EUV exposures on thin films (~60 nm) coated onto silicon wafers. The term open-frame refers to an exposure arrangement whereby the coated wafer is placed directly in the beam path with no mask present. In some cases, the wafers then underwent a post-exposure bake (PEB) step whereby the wafer was heated at 70 °C for 60 s prior to development. The irradiated wafers were then developed using an organic solvent (see Table 2) to remove low molecular weight scission products. Following development, the thickness of the remaining film at each exposure dose was measured *via* ellipsometery and the $E_0$ value, defined as the lowest dose at which the film is cleared to the wafer, was determined and used as a measure of the sensitivity of the resist.

Initial studies were conducted investigating suitable combinations of developing solvents. Developers containing various ratios of isopropyl alcohol (IPA) and methylisobutylketone (MIBK) were investigated because the unirradiated polymer is not soluble in IPA but is soluble in MIBK. Thus there will be an optimal ratio of IPA/MIBK for solubilising the low molecular weight degradation products, but not removing the higher molecular weight unirradiated regions. The $E_0$ values obtained from these studies can be seen in Table 2. It can be seen that the homopolymer (**2**) has a lower $E_0$ (and thus a higher sensitivity) than the terpolymers (**3a**) and (**3b**) when 100% IPA developer is used, but as the MIBK content is increased this trend is reversed. This suggests that the sulfone backbone is being degraded preferentially, since 2.7k PMMA arms that are covalently attached to a higher molecular weight backbone are not expected to be solubilised until more MIBK is included in the developer.

Also in Table 2 it can be seen that the highest sensitivity for materials (**2**) and (**3a–b**) was observed when using a 70/30 IPA/MIBK developer combination. A slight increase in sensitivity was observed using this developer when a PEB step was performed (Table 2). Since these conditions gave the best results, they were used to investigate the sensitivity of materials (**3c**) and (**3d**). Only one developer combination was trialed for these materials because only limited amounts of the materials were available.

Traditional chain-scission materials such as PMMA require doses in the range 150–550 mJ cm$^{-2}$ to achieve patterning[28] when irradiated with EUV photons, however, recently a number of polycarbonate-based chain scission resist materials were reported with $E_0$ values of 37–56 mJ cm$^{-2}$.[29] The high sensitivity

**Table 2** $E_0$ values obtained for materials when using different developer combinations

| Material | 100% IPA/mJ cm$^{-2}$ | 90/10 IPA/MIBK/mJ cm$^{-2}$ | 80/20 IPA/MIBK/mJ cm$^{-2}$ | 70/30 IPA/MIBK/mJ cm$^{-2}$ |
|---|---|---|---|---|
| **(2)** | 132.4 | 95.3 | 57.1 | 6.2, 5.8[a] |
| **(3a)** | 269.0 | 87.2 | 50.9 | 6.1, 5.7[a] |
| **(3b)** | 282.9 | 82.1 | 53.3 | 4.9, 4.6[a] |
| **(3c)** | — | — | — | 5.4[a] |
| **(3d)** | — | — | — | 5.4[a] |

[a] Wafers underwent a post-exposure bake (PEB) of 70 °C for 60 s following exposure and prior to development.

observed for the terpolymer materials suggests that the poly(olefin sulfone) backbone is undergoing depolymerisation under the high vacuum conditions during irradiation. Similar results have been reported previously for poly(1-pentene sulfone) and poly(2-methyl-1-pentene sulfone).[21] This suggests that poly(olefin sulfone)s are chain scission resist materials capable of meeting the sensitivity target requirements of <10 mJ cm$^{-2}$ set for EUV lithography.[30] The contrast curves, *i.e.* plots of film thickness *versus* the log of the exposure dose after a solvent development step, for material (**3b**) are shown in Fig. 2(A). Analogous curves were obtained for materials (**2**) and (**3a**) (see ESI†). From these figures it is apparent that despite generating the highest sensitivity, the developer of 70/30 IPA/MIBK causes the film to swell as evidenced by the normalised film thickness being greater than 1 at low doses. This indicates that further optimisation of developer is necessary for use in pattering experiments, in order to maximise the sensitivity of the poly(olefin sulfone) backbone while preventing swelling during development.

Fig. 2(B) shows the contrast curves for all materials ((**2**) and (**3a–d**)) obtained using 70/30 IPA/MIBK as a developer. Materials (**3c**) and (**3d**) were found to possess poor coating properties, where visible defects were present in the coated films. Evidence of this can be seen in the thickness variation observed in the contrast curves for these materials (Fig. 2). Also from this figure it can be seen that the level of incorporation of PMMA (materials (**3a**) and (**3b**)) and the molecular weight of the incorporated PMMA arms (materials (**3a–d**)) do not affect the observed $E_0$ values. This indicates that even at relatively high incorporations of PMMA, such as in material (**3b**), the high sensitivity of the sulfone backbone is maintained.

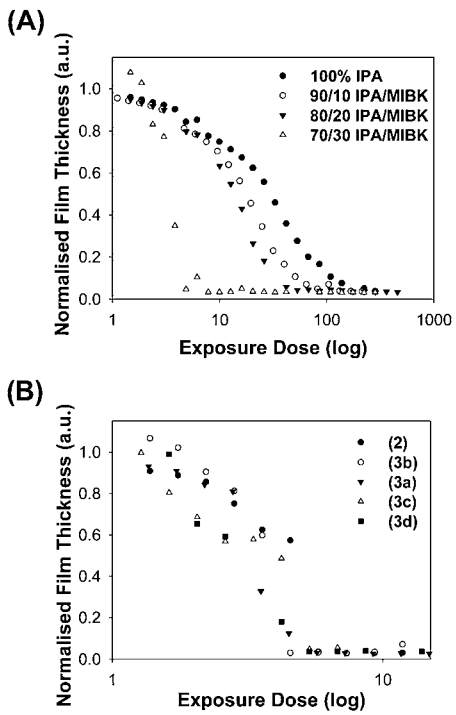


**Fig. 2** (A) Contrast curves with different developer combinations for 60 nm thick films of material (**3a**); no post-exposure bake (PEB) was conducted and all samples were developed for 45 s followed by a spin drying step. (B) Contrast curves for 60 nm thick films of materials (**2**) and (**3a–d**); wafers underwent a post-exposure bake (PEB, 70 °C for 60 s) following irradiation and were developed with 70/30 IPA/MIBK for 45 s.

***In situ* headspace analysis studies.** In order to gain insights into the degradation behaviour of resist materials under EUV irradiation, the levels and types of species evolved into the headspace during irradiation were investigated by measuring mass spectra of the emitted species as a function of dose. Fig. 3 shows the outgassing rate of fragments as function of mass/charge ratios (*m*/*z*) for samples of the homopolymer (**2**) and the terpolymer (**3b**) that were irradiated with EUV photons to a dose of 400 mJ cm$^{-2}$. The plots show that both materials exhibited significant loss of small molecules derived from the parent monomers $SO_2$ and 1-pentene (Fig. 4) during irradiation. No fragment peaks are observed for the reported photodegradation products of PMMA,[31] suggesting that the sulfone backbone is undergoing preferential degradation.

Further evidence for the preferential degradation of the polysulfone backbone was obtained using grazing-angle total attenuated reflectance FTIR (GATR-FTIR). GATR allows the FTIR spectra of ultrathin films (<60 nm) on silicon wafers to be acquired with high sensitivity, due to the enhanced electric field that occurs between the germanium internal reflective element and the silicon wafer. This enhancement occurs due to the grazing angle conditions and the high refractive index of the silicon wafer and germanium internal reflective element.[32] The GATR-FTIR spectra of wafers coated with poly(pentene sulfone), material (**3b**) which has been irradiated with EUV photons to a dose of ~300 mJ cm$^{-2}$ and 2.7k PMMA are shown in Fig. 4. The spectra of the polysulfones (**2**) and (**3b**) exhibit peaks at 1125 cm$^{-1}$ and 1300 cm$^{-1}$, which are characteristic for other polysulfones reported in the literature[15,33] and can be assigned to symmetric and asymmetric –$SO_2$– stretching vibrations, respectively.[34] It can be seen that the peaks corresponding to –$SO_2$– stretching vibrations significantly decrease following irradiation, while those corresponding to the PMMA component of the material remain unchanged (Fig. 4). Finally it is noted that the preferential degradation of the poly(olefin sulfone) backbone

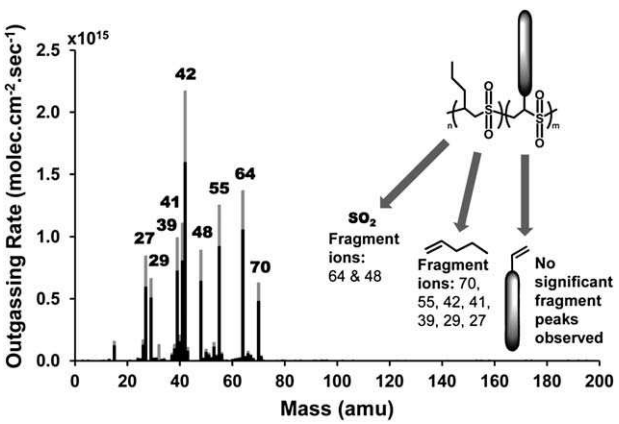


**Fig. 3** Mass spectral traces for volatile species produced from the EUV photodegradation of (**2**), poly(1-pentene sulfone) (grey), and material (**3b**) (23 wt% 2.7k PMMA containing terpolymer) (black). Peaks corresponding to $SO_2$ (64 and 48 *m*/*z*) and 1-pentene (peaks at 70, 55, 42, 41, 39, 29, 27 *m*/*z*) are indicated.

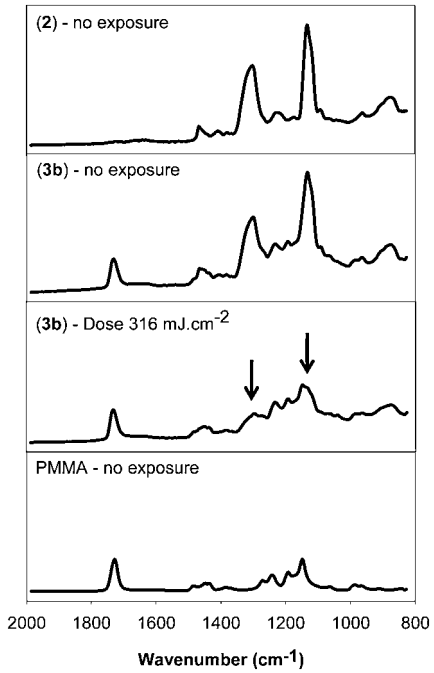


**Fig. 4** GATR spectra of poly(1-pentene sulfone) (**2**) and terpolymer material (**3b**) prior to and following irradiation with EUV photons to a dose of 316 mJ $cm^{-2}$. Arrows indicate a decrease in the sulfone peaks as a result of irradiation. A PMMA spectrum was included for comparison.

provides a handle to tune the further development of the system because the solubility properties of the arms will be the major factor influencing development.

**EUV patterning.** EUV patterning was performed on materials (**2**), (**3a**) and (**3b**) using an EUV interference lithography setup described previously.[28] Materials (**3c**) and (**3d**) were excluded from the study due to their poor coating properties. The developer selected for patterning studies was 90/10 IPA/MIBK, because this developer did not cause swelling of the unirradiated resist, while the 70/30 IPA/MIBK developer, which exhibited better sensitivity also exhibited an unacceptable degree of swelling (Fig. 2). Because of this, the doses required for patterning are increased. Thus, it is necessary to further optimise developer–resist interactions and such studies are underway in our laboratory. Using 90/10 IPA/MIBK the $E_0$ values found for materials (**2**), (**3a**) and (**3b**) were 95.3 mJ $cm^{-2}$, 87.2 mJ $cm^{-2}$ and 82.1 mJ $cm^{-2}$, respectively (Table 2).

Initial attempts to investigate the patterned features using scanning electron microscopy (SEM) were unsuccessful because severe electron beam damage was observed, resulting in poor quality images (see ESI†). This high sensitivity to electrons may make these polymers useful for additional next-generation lithography platforms, such as self-powered electron lithography[35] or multiple-beam-electron direct write lithography.[36] In order to overcome the difficulties observed during SEM measurements, atomic force microscopy (AFM) was explored as an alternative imaging technique. Low magnification SEM was first used to select the exposure fields, which had received sufficient dose to clear the resist. It was found that the $E_{size}$, the dose to clear for a particular line space size, for the materials were lower than expected. It is generally observed that for chemically amplified materials $E_{size}$ is higher than the corresponding $E_0$, however, lower than expected $E_{size}$ values have been observed previously for non-CAR materials.[29]

AFM images of patterns in the materials at similar doses can be seen in Fig. 5. From these images it can be seen that all materials achieve reasonable patterning down to 30 nm half-pitch (Fig. 5, images B, E and H). The critical dimensions (CD), the resolvable distance between lines, for the 1 : 1 line space patterns were determined by Fast Fourier Transform (FFT) analysis on the images and obtaining the average period which is assigned to the pitch (the distance of a line-space pair); The CD is then half of this value. It can be seen that the CD is close to that predicted from the mask dimensions indicating that the materials are capable of accurate pattern transfer for 30 nm and 50 nm lines and spaces.

For the 22.5 nm lines and spaces, materials (**2**) and (**3a**) exhibited poor resolution, with the major failure mechanisms being bridging and pattern collapse (Fig. 5, images C and F). There is also evidence of delamination of the resist from the wafer, possibly due to poor adhesion to the silicon. It is also possible that the poor resolution observed is due to swelling of the materials in the developer solution as observed in the contrast curves (Fig. 2) when 70/30 IPA/MIBK was used as a developer. The 22.5 nm patterns are better resolved for material (**3b**), with only minor pattern collapse which indicates that PMMA macromonomer that has been incorporated into the polymer is resulting in greater structural integrity of the resulting patterns.

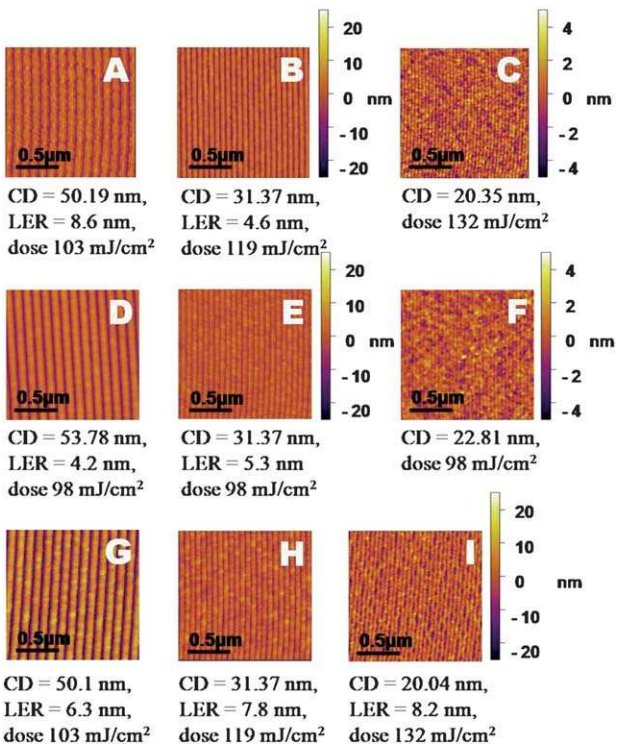


**Fig. 5** AFM height images of 1 : 1 line-space patterns for materials (**2**) (images A–C), (**3a**) (images D–F) and (**3b**) (images G–I) showing at resolutions of 50 nm, 30 nm and 22.5 nm half-pitch. The corresponding critical dimensions (CD), LER and dose to resist are shown on the images.

Some of the collapse observed for all materials is likely due to the fact that the films are quite thick (60 nm) leading to an aspect ratio of 3 which is at the limit of the capabilities of typical resists.[3]

The LER values observed for the materials compare well to values measured for a range of chemically amplified EUV resist materials using the same interference patterning system where LER values in the range 3.5–12.6 nm were recorded for line spaces with a half-pitch of 25–50 nm.[37] A trend of increasing LER with increasing PMMA incorporation is observed (Fig. 5). Chen *et al.*[38] have reported that incorporation of allyl monomers into poly(olefin sulfones) results in inhibition of depolymerisation reactions that occur following irradiation with 193 nm photons. Hence, it is possible that incorporation of the PMMA arms increases LER by inhibiting the depolymerisation reaction. If complete depolymerisation is occurring in irradiated areas it is expected that the line edges would be relatively sharp. However, if the presence of a PMMA arm halts the depolymerisation reaction then this would result in larger sections of polymer remaining to be developed out and generate increased roughness in the line edges. Further investigation of this effect and identification of monomers that do not inhibit the depolymerisation reaction are currently in progress in our labs.

## Conclusions

A series of novel chain scissioning resist polymers with a comb architecture were prepared having a highly degradable poly(1-pentene sulfone) backbone and PMMA arms that have been incorporated with the aim to improve structural stability. The polymers were extensively characterised in terms of their physical properties and have undergone preliminary lithographic characterisation. Open-frame EUV exposures showed that the materials possess excellent sensitivity towards degradation by EUV radiation, having open frame sensitivities in the range 4–6 mJ $cm^{-2}$. This is within the target range for EUV resist materials and is, to the best of our knowledge, the highest sensitivity observed to date for a chain scission EUV resist material. Varying the molecular weight and percentage incorporation of the PMMA arms was found not to affect the sensitivity of the materials, however, materials containing high molecular weight arms were found to have poor coating properties.

Headspace mass spectrometry studies showed that the poly(olefin sulfone) backbone undergoes preferential photodegradation followed by depolymerisation when irradiated under vacuum conditions. This observation was supported by GATR-FTIR studies which showed peaks corresponding to PMMA remained following irradiation with EUV photons while those corresponding to the poly(olefin sulfone) backbone decreased.

EUV patterning studies showed that all materials were capable of resolving 1 : 1 line : space patterns of 30 nm, while the material containing a high incorporation of PMMA arms exhibited improved patterning performance at a resolution of 22.5 nm half-pitch compared to poly(1-pentene sulfone) and terpolymers with a low incorporation of PMMA. This increase in integrity shows that the incorporation of a third monomer unit into a poly(olefin sulfone) backbone has the potential to provide a highly sensitive, tunable materials platform for chain scission based EUV lithography resists.

## Acknowledgements

This research was supported in part by the Intel Corporation and under the Australian Research Council Linkage Projects funding scheme (project number LP0989607). Exposures were performed on the soft X-ray beamline at the Australian Synchrotron, Victoria, Australia. In addition, characterisation was performed at the Queensland node of the Australian National Fabrication Facility. KJL would like to thank the Katholieke Universiteit Leuven (KUL) for funding which allowed part of this work to be conducted at imec, Leuven, Belgium. The authors would like to acknowledge Mr Craig Bell, Dr Andreas Langer, Dr Lauren Butler, Dr Bogdan Donose, Dr Bruce Cowie, Dr Lars Thomsen and Dr Elena Taran for assistance with obtaining the results presented.

## References

1 G. L. Timothy, M. Z. Aasiyeh and H. G. David, *Small*, 2010, **6**, 792.
2 D. Mark, S. Haeberle, G. Roth, F. v. Stetten and R. Zengerle, *Chem. Soc. Rev.*, 2010, **39**, 1153.
3 ITRS, International Technology Roadmap for Semiconductors 2007 Edition, http://www.itrs.net/, accessed November, 2008.
4 T. Honda, Y. Kishikawa, Y. Iwasaki, A. Ohkubo, M. Kawashima and M. Yoshii, *Proc. SPIE*, 2006, **6154**, 615422; G. M. Schmid, M. D. Stewart, C.-Y. Wang, B. D. Vogt, V. M. Prabhu, E. K. Lin and C. G. Willson, *Proc. SPIE*, 2004, **5376**, 333.
5 M. D. Stewart, H. V. Tran, G. M. Schmid, T. B. Stachowiak, D. J. Becker and C. G. Willson, *J. Vac. Sci. Technol., B*, 2002, **20**, 2946.
6 R. L. Bristol, *Proc. SPIE*, 2007, **6519**, 65190W; R. L. Brainard, P. Trefonas, J. H. Lammers, C. A. Cutler, J. F. Mackevich, A. Trefonas and S. A. Robertson, *Proc. SPIE*, 2004, **5374**, 74.
7 A. R. Neureuther, R. F. W. Pease, L. Yuan, K. B. Parizi, H. Esfandyarpour, W. J. Poppe, J. A. Liddle and E. H. Anderson, *J. Vac. Sci. Technol., B*, 2006, **24**, 1902; D. Van Steenwinckel, J. H. Lammers, L. H. A. Leunissen and J. A. J. M. Kwinten, *Proc. SPIE*, 2005, **5753**, 269; G. M. Gallatin, *Proc. SPIE*, 2004, **5754**, 38.
8 G. M. Gallatin, P. Naulleau and R. Brainard, *Proc. SPIE*, 2007, **6519**, 651911/1; G. M. Gallatin, P. Naulleau, D. Niakoula, R. Brainard, E. Hassanein, R. Matyi, J. Thackeray, K. Spear and K. Dean, *Proc. SPIE*, 2008, **6921**, 69211E; P. P. Naulleau, C. Rammeloo, J. P. Cain, K. Dean, P. Denham, K. A. Goldberg, B. Hoef, B. La Fontaine, A. R. Pawloski, C. Larson and G. Wallraff, *Proc. SPIE*, 2006, **6151**, 61510Y; D. Van Steenwinckel, R. Gronheid, J. H. Lammers, A. M. Meyers, F. Van Roey and P. Willems, *Proc. SPIE*, 2007, **6519**, 65190V.
9 N. Isao, H. H. William, M. Kazuya, J. Wei-Lun, S. L. Saul, N. Colin, S. Tsutomu, I. Koji, F. Koichi and C. G. Willson, *Proc. SPIE*, 2008, **6923**, 69231C; T. Ito, A. Terao, Y. Inao, T. Yamaguchi and N. Mizutani, *Proc. SPIE*, 2007, **6519**, 65190J; A. Aviram, M. Angelopoulos, E. Babich, I. Babich, K. Petrillo and D. Seeger, *Proc. SPIE*, 1998, **3331**, 349.
10 K. Jack, H. Liu, I. Blakey, D. Hill, Y. Wang, H. Cao, M. Leeson, G. Denbeaux, J. Waterman and A. Whittaker, *Proc. SPIE*, 2007, **6519**, 65193Z.
11 I. Blakey, A. Yu, J. Blinco, K. S. Jack, H. Liu, M. J. Leeson, W. Yueh, T. Younkin and A. K. Whittaker, *Proc. SPIE*, 2010, **7636**, 763635.
12 T. Kozawa and S. Tagawa, *Appl. Phys. Express*, 2009, **2**, 095004.
13 M. J. Bowden and J. H. O'Donnell, *Dev. Polym. Degrad.*, 1985, **6**, 21.
14 T. N. Bowmer and J. H. O'Donnell, *Polym. Degrad. Stab.*, 1981, **3**, 87.
15 R. E. Cook, F. S. Dainton and K. J. Ivin, *J. Polym. Sci.*, 1957, **26**, 351.
16 L. F. Thompson and M. J. Bowden, *J. Electrochem. Soc.*, 1973, **120**, 1722; T. R. Pampalone, *J. Imaging Sci.*, 1986, **30**, 160; A. S. Gozdz, H. G. Craighead and M. J. Bowden, *Polym. Eng. Sci.*, 1986, **26**, 1123.
17 E. Gipstein, W. Moreau, G. Chiu and O. U. Need, III, *J. Appl. Polym. Sci.*, 1977, **21**, 677.
18 M. Matsuda and H. Ono, JP-63000319-A, 1988; M. Matsuda, *US Pat.*, 4965340-A, 1990; R. J. Himics, N. V. Desai, M. Kaplan and E. S. Poliniak, *Polym. Prepr.*, 1975, **35**, 266; H. Ito, *IBM J. Res. Dev.*, 2001, **45**, 683; M. J. Bowden, A. S. Gozdz, J. M. DeSimone,

 

J. E. McGrath, S. Ito and M. Matsuda, *Makromol. Chem., Macromol. Symp.*, 1992, **53**, 125.
19 B. Serre and D. J. Worsfold, *Polymer*, 1987, **28**, 881; G. Laivins and D. J. Worsfold, *J. Polym. Sci., Part A: Polym. Chem.*, 1990, **28**, 1413; J. M. DeSimone, J. E. McGrath and S. D. Smith, *Polym. Prepr.*, 1988, **29**, 345.
20 J. M. DeSimone, G. A. York, J. E. McGrath, A. S. Gozdz and M. J. Bowden, *Macromolecules*, 1991, **24**, 5330.
21 K. Lawrie, I. Blakey, J. Blinco, R. Gronheid, K. Jack, I. Pollentier, M. Leeson, T. Younkin and A. Whittaker, *Radiat. Phys. Chem.*, 2011, **80**, 236.
22 D. M. Haddleton, M. C. Crossman, B. H. Dana, D. J. Duncalf, A. M. Heming, D. Kukulj and A. J. Shooter, *Macromolecules*, 1999, **32**, 2110.
23 I. Pollentier, G. Aksenov, A. M. Goethals, R. Gronheid, R. Jonckheere and M. Leeson, *Proc. SPIE*, 2009, **7271**, 727146.
24 H. H. Solak, C. David, J. Gobrecht, V. Golovkina, F. Cerrina, S. O. Kim and P. F. Nealey, *Microelectron. Eng.*, 2003, **67–68**, 56.
25 N. Tokura, *Encycl. Polym. Sci. Technol.*, 1968, **9**, 460.
26 Z. Florjanczyk and E. Zygadlo, *Makromol. Chem.*, 1991, **192**, 1881.
27 Z. Florjanczyk, T. Florianczyk and B. B. Klopotek, *Makromol. Chem.*, 1987, **188**, 2811.
28 R. Gronheid, H. H. Solak, Y. Ekinci, A. Jouve and F. Van Roey, *Microelectron. Eng.*, 2006, **83**, 1103.
29 A. Yu, H. Liu, J. P. Blinco, K. S. Jack, M. Leeson, T. R. Younkin, A. K. Whittaker and I. Blakey, *Macromol.Rapid Commun.*, 2010, **31**, 1449.
30 S. E. Putna, T. R. Younkin, R. Caudillo and M. Chandhok, *Proc. SPIE*, 2010, **7636**, 76360P.
31 M. C. K. Tinone, K. Tanaka and N. Ueno, *J. Vac. Sci. Technol., A*, 1995, **13**, 1885.
32 M. Milosevic, V. Milosevic and S. L. Berets, *Appl. Spectrosc.*, 2007, **61**, 530.
33 I. Ito, H. Hayashi, T. Saigusa and J. Furukawa, *Makromol. Chem.*, 1962, **55**, 15.
34 D. H. Williams and I. Flemming, *Spectroscopic Methods in Organic Chemistry*, London, Sydney, McGraw-Hill, 1995.
35 Y. Lu and A. Lal, *Nano Lett.*, 2010, **10**, 2197.
36 S.-Y. Chen, S.-C. Chen, H.-H. Chen, K.-Y. Tsai and H.-H. Pan, *Jpn. J. Appl. Phys.*, 2010, **49**, E05.
37 R. Gronheid and M. J. Leeson, *J. Micro/Nanolithogr., MEMS, MOEMS*, 2009, **8**, 021205/1.
38 L. Chen, Y.-K. Goh, K. Lawrie, B. Smith, W. Montgomery, P. A. Zimmerman, I. Blakey and A. K. Whittaker, *Proc. SPIE*, 2010, **7639**, 76390V/1; L. Chen, G. Yong-Keng, K. Lawrie, Y.-M. Chuang, E. Piscani, P. A. Zimmerman, I. Blakey and A. K. Whittaker, *Radiat. Phys. Chem.*, 2011, **80**, 242.